

AD-A032 046

NAVAL RESEARCH LAB WASHINGTON D C  
NUMERICAL SOLUTION OF THE PARABOLIC EQUATION WITH THE PEP CODE. (U)  
OCT 76 B E MCDONALD  
NRL-MR-3385

F/G 20/14

UNCLASSIFIED

NL

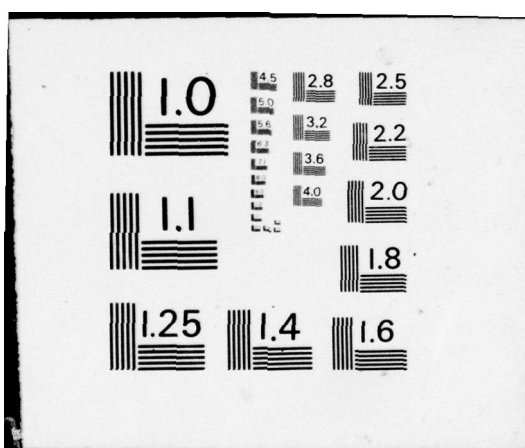
1 OF 1  
ADA032046



END

DATE  
FILMED

1 - 77



AD A 0 32046

(12)

NRL Memorandum Report 3385

J  
J

## Numerical Solution of the Parabolic Equation with the PEP Code

B. E. McDONALD

*Plasma Dynamics Branch  
Plasma Physics Division*

October 1976



D D C  
RECORDED  
NOV 16 1976  
J  
J  
RECORDED  
C

NAVAL RESEARCH LABORATORY  
Washington, D.C.

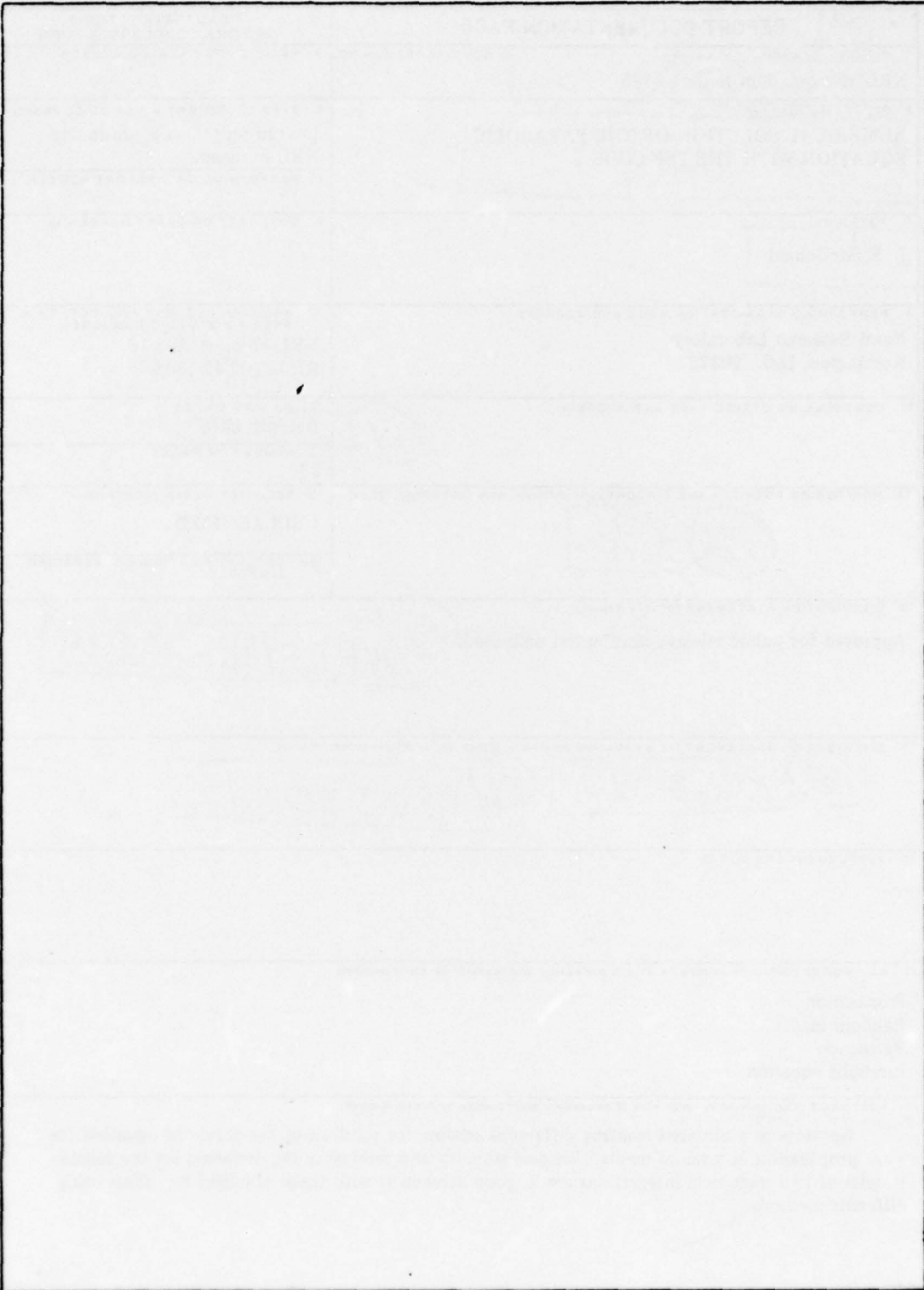
Approved for public release; distribution unlimited.

## SECURITY CLASSIFICATION OF THIS PAGE (When Data Entered)

REPORT DOCUMENTATION PAGE		READ INSTRUCTIONS BEFORE COMPLETING FORM
1. REPORT NUMBER NRL Memorandum Report 3385	2. GOVT ACCESSION NO.	3. RECIPIENT'S CATALOG NUMBER
4. TITLE (and Subtitle) NUMERICAL SOLUTION OF THE PARABOLIC EQUATION WITH THE PEP CODE		5. TYPE OF REPORT & PERIOD COVERED Interim report on a continuing NRL problem.
6. AUTHOR(S) B. E. McDonald		7. PERFORMING ORGANIZATION NAME AND ADDRESS Naval Research Laboratory Washington, D.C. 20375
8. CONTRACT OR GRANT NUMBER(S)		9. PROGRAM ELEMENT, PROJECT, TASK AREA & WORK UNIT NUMBERS NRL Problem A03-16 RR033-02-42-5308
10. CONTROLLING OFFICE NAME AND ADDRESS		11. REPORT DATE October 1976
12. MONITORING AGENCY NAME & ADDRESS(if different from Controlling Office) 1219P.		13. NUMBER OF PAGES 22
14. DISTRIBUTION STATEMENT (of this Report) Approved for public release; distribution unlimited.		15. SECURITY CLASS. (of this report) UNCLASSIFIED
16. DISTRIBUTION STATEMENT (of the abstract entered in Block 20, if different from Report) 16 RR03302		17. DECLASSIFICATION/DOWNGRADING SCHEDULE 17 RR0330242
18. SUPPLEMENTARY NOTES		
19. KEY WORDS (Continue on reverse side if necessary and identify by block number) Propagation Random media Refraction Parabolic equation		
20. ABSTRACT (Continue on reverse side if necessary and identify by block number) Proposed We propose a centered leapfrog difference scheme for solution of the parabolic equation for wave propagation in random media. We give stability and resolution requirements for the scheme. Results of two numerical integrations are in good agreement with those obtained by others using different methods.		

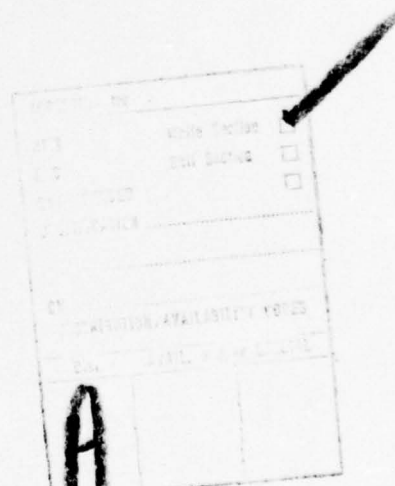
251950 LB

SECURITY CLASSIFICATION OF THIS PAGE(When Data Entered)



## CONTENTS

1. THE WAVE EQUATION .....	1
2. THE PARABOLIC APPROXIMATION .....	3
3. NUMERICAL INTEGRATION OF THE PARABOLIC EQUATION .....	4
A. FINITE DIFFERENCE SCHEME .....	4
B. STABILITY ANALYSIS .....	5
C. BOUNDARY CONDITIONS .....	8
D. RESULTS FROM THE PEP CODE .....	9
SUMMARY .....	11
REFERENCES .....	13



## NUMERICAL SOLUTION OF THE PARABOLIC EQUATION WITH THE PEP CODE

### 1. THE WAVE EQUATION

We are concerned with obtaining numerical solutions to the three-dimensional wave equation

$$[\nabla^2 + k_0^2 (1 + \chi(\tilde{r}))] E(\tilde{r}) = 0 \quad (1)$$

in a region of space where the index of refraction varies slowly with  $\tilde{r}$ . Subject to certain assumptions, (1) describes radio propagation through a spatially varying plasma<sup>1</sup>, or acoustic wave propagation through a medium in which the sound speed is a function of space<sup>2</sup>. The solution  $E$  is assumed to have a time dependence  $e^{i\omega t}$ , and the wave-number  $k_0$  is  $\omega/c$ , where  $c$  is the speed of light for the radio application, or a reference sound speed for the acoustic application.

For radio wave propagation,  $E(\tilde{r})$  is a scalar component of the electric field, and  $\chi(\tilde{r})$  is the known electric susceptibility of the plasma. Equation (1) neglects a depolarization term whose magnitude is approximately  $k_0 |E\nabla\chi|$  for small  $\chi$ . If  $\chi$  varies on a length scale  $L$ , the depolarization term is smaller than the  $k_0^2 \chi$  term of (1) by a factor  $1/k_0 L$ . We shall be interested in applications in which  $L \gg 1/k_0$ , so the depolarization term is expected to be negligible. The use of a scalar  $\chi$  also assumes implicitly that magnetization is unimportant; namely, that  $\omega$  is much greater than the electron cyclotron frequency.

For acoustic applications,  $E$  is the sound pressure, and  $\chi$  is a measure of the sound speed fluctuation such that the local sound speed

Note: Manuscript submitted September 20, 1976.

is  $c\sqrt{1 + \chi(\xi)}$ . Just as in the radio wave application, a term involving the gradient of  $\chi$  has been neglected, but again, its magnitude is down from that of the  $\chi k_o^2$  term by a factor  $1/k_o L$ .

For solutions of (1), let us make the substitution

$$E(\xi) = u(\xi) e^{i \int k(z) dz}, \quad (2)$$

where

$$k(z) = k_o \sqrt{1 + \chi_o(z)}, \quad (3)$$

and  $\chi_o(z)$  is some "background"  $\chi$  profile along an assumed propagation direction  $z$ . The geometry of the problem is illustrated in Figure 1. For reasons of computational efficiency to be demonstrated later, (2) is in some cases preferable to a more standard approach<sup>3,4</sup> in which the phase factor is taken to be  $e^{ik_o z}$ . Substitution of (2) into (1) gives

$$\nabla^2 u + 2ik(z) \partial_z u + u(i\partial_z k + k_o^2 \chi_1) = 0 \quad (4)$$

where

$$\chi_1(\xi) = \chi(\xi) - \chi_o(z). \quad (5)$$

One further transformation is useful before introducing the parabolic approximation: let

$$f(\xi) = u(\xi) (k/k_o)^{\frac{1}{2}} \quad (6)$$

$$= u(\xi) (1 + \chi_o(z))^{\frac{1}{4}}.$$

Thus  $E(\xi) = f(\xi) (1 + \chi_o(z))^{-\frac{1}{4}} e^{i \int k(z) dz}.$  (7)

Then (4) becomes

$$\nabla_{\perp}^2 f + k^{\frac{1}{2}} \partial_z^2 (fk^{-\frac{1}{2}}) + 2ik \partial_z f + fk_o^2 \chi_1 = 0, \quad (8)$$

Where  $\perp$  refers to the two Cartesian coordinates  $x$  and  $y$  orthogonal to  $z$ . It is important to note that no approximations have been introduced

between (1) and (8).

## 2. THE PARABOLIC APPROXIMATION

If we assume that  $f$  is substantially constant over a distance of one wavelength

$$\lambda = 2\pi/k_0 , \quad (9)$$

$$\text{and that } |\chi_1| \ll 1 , \quad (10)$$

the second  $z$  derivative in (8) becomes negligible in comparison with the first  $z$  derivative. To define what "negligible" means, let us assume that  $f$  varies on a length scale  $L \gg \lambda$  and assign constant values to  $k$  and  $\chi_1$ . We Fourier transform  $f$  according to

$$f(\tilde{z}) = \int \tilde{f}(\tilde{P}) e^{i\tilde{P} \cdot \tilde{z}} d\tilde{P} . \quad (11)$$

The transform of (8) then gives

$$-P_{\perp}^2 - P_z^2 - 2k P_z + k_0^2 \chi_1 = 0 . \quad (12)$$

Because of the slow variation assumed for  $f$ , we can assign a limiting value to  $P_{\perp}$ :

$$P_{\perp}^2 \ll 1/L^2 . \quad (13)$$

If we take  $k \approx k_0$ , (12) and (13) give a limiting value for  $P_z$ :

$$\left( \frac{P_z}{k_0} \right)^2 + 2 \frac{P_z}{k_0} \rightarrow \chi_1 - \frac{1}{k_0^2 L^2} . \quad (14)$$

The right side of (14) is small by assumption, so

$$\frac{P_z}{k_0} \rightarrow \frac{1}{2} \left( \chi_1 - \frac{1}{k_0^2 L^2} \right) + O\left( \left( \chi_1 - \frac{1}{k_0^2 L^2} \right)^2 \right) \quad (15)$$

Since the quadratic term can be dropped from (14), the second  $z$

derivative may be dropped from (8):

$$\partial_z f = \frac{i}{2k} (\nabla_{\perp}^2 f + k_o^2 \chi_1 f) . \quad (16)$$

This is the "parabolic equation" for  $f$ . The fractional error in  $f$  resulting from the parabolic approximation is on the order of

$$|\chi_1 - \frac{1}{k_o^2 L^2}| .$$

### 3. NUMERICAL INTEGRATION OF THE PARABOLIC EQUATION

Note that (16) represents an initial value problem with regard to  $z$  integration. We can specify  $f$  at some initial  $z$  to describe an incident wave, and use (16) to step through a region of arbitrarily varying  $\chi_1$ . Previous numerical application of the parabolic equation to the ionospheric scintillation problem has been primarily oriented toward propagation into free space of a wave which has just emerged from a random phase screen<sup>4</sup>. In this application, one Fourier transforms the initial  $f(x,y,o)$ , advances the phase of each spectral component in an appropriate way, and then transforms back to get  $f(x,y,z)$ . However, by integrating (16) within the scattering medium, one can follow the growth of amplitude and phase variations in an arbitrarily thick slab.

#### A. FINITE DIFFERENCE SCHEME

We propose a leapfrog scheme to integrate (16), with real and imaginary parts of  $f$  defined on alternate  $z$  levels (see Figure 2).

Let us express  $f$  explicitly in terms of real and imaginary parts:

$$f(\underline{r}) = f_r(\underline{r}) + i f_i(\underline{r}) \quad (17)$$

where  $f_r$  and  $f_i$  are real. Then (16) gives the coupled linear system:

$$\partial_z f_r = \frac{-1}{2k} \left( \nabla_{\perp}^2 f_i + k_o^2 \chi_1 f_i \right) \quad (18)$$

$$\partial_z f_i = \frac{1}{2k} \left( \nabla_{\perp}^2 f_r + k_o^2 \chi_1 f_r \right).$$

This system may be integrated on a staggered mesh, with  $f_r$  and  $f_i$  defined on alternate  $z$  levels. The three functions  $f_r$ ,  $f_i$ , and  $\chi_1$  are discretized in  $(x, y, z)$  space with integer indices  $(I, J, K)$ . The mesh spacings in the  $x$  and  $y$  directions are the same value,  $\delta x$ ; the spacing between the  $z$  planes is  $\delta z$ . We shall use the following second order difference formulas:

$$\partial_z f(k) \rightarrow \frac{f(k+1) - f(k-1)}{2\delta z} \quad (19)$$

$$\nabla_{\perp}^2 f(I, J, K) \rightarrow [f(I+1, J, K) + f(I-1, J, K) \\ + f(I, J+1, K) + f(I, J-1, K) - 4f(I, J, K)]/\delta x^2$$

## B. STABILITY ANALYSIS

If an additive error  $\epsilon = \epsilon_r + i \epsilon_i$  is introduced into a discretized solution  $f$ , then  $\epsilon$  itself must satisfy (18). This error may be Fourier analyzed, and stability analysis applied to each spectral component. We take  $\chi_1$  constant, set  $k = k_o$  for simplicity, and take

$$\epsilon(\underline{r}) \propto e^{i(P_x X + P_y Y + P_z Z)} \quad (20)$$

For a specific choice of  $(P_x, P_y, P_z)$ , the derivative operators  $\partial_z$  and  $\nabla_{\perp}^2$  may be treated as algebraic multipliers. Substitution of (20) into (16) gives

$$\partial_z = \frac{1}{2k_0} (\nabla_{\perp}^2 + k_0^2 \chi_{\perp}), \quad (21)$$

where

$$\begin{aligned} \partial_z &= \frac{e^{iP_z \delta z} - e^{-iP_z \delta z}}{2\delta z} \\ &= i \sin(P_z \delta z) / \delta z, \end{aligned} \quad (22)$$

$$\text{and } \nabla_{\perp}^2 = -\frac{2}{\delta x^2} [2 - \cos(P_x \delta x) - \cos(P_y \delta x)] \quad (23)$$

For investigating stability of integrating forward in the  $z$  direction, we set

$$\gamma = e^{iP_z \delta z}. \quad (24)$$

The stability criterion will be  $|\gamma| \leq 1$ . Now (21) gives the quadratic equation

$$\gamma - \gamma^{-1} = i\mu, \quad (25)$$

where

$$\mu = \frac{\delta z}{k_0} \left( \nabla_{\perp}^2 + k_0^2 \chi_{\perp} \right). \quad (26)$$

The solution to (25) is

$$\gamma = i\frac{\mu}{2} \pm \sqrt{1 - \frac{\mu^2}{4}} \quad (27)$$

When  $\mu^2/4 > 1$ , one of the roots gives  $|\gamma| > 1$ , and the scheme is unstable. When  $\mu^2/4 \leq 1$ , the radical in (27) is real, and

$$|\gamma|^2 = \left(\frac{\mu}{2}\right)^2 + (1 - \frac{\mu^2}{4}) = 1. \quad (28)$$

Thus the stability criterion is

$$|\mu| \leq 2 \quad (29)$$

The greatest possible value of  $|\mu|$  occurs when  $\nabla_{\perp}^2 = -8/\delta x^2$ , and

$x_1 < 0$ . Thus all modes are stable when the following is satisfied:

$$\text{STABILITY REQUIREMENT: } \delta z \leq \frac{2k_o}{8/\delta x^2 + k_o^2 |x_1|} . \quad (30)$$

This criterion demonstrates the advantage of separating the background  $x_o$  from the fluctuations  $x_1$ . If we had used  $e^{ik_o z}$  as a phase factor in (2), then  $x_1$  in (30) would be replaced by  $x_o + x_1$ . In typical applications, this would result in a smaller stepsize  $\delta z$ .

In addition to the stability criterion (30) we wish also to impose a resolution requirement that  $\delta z$  change by only a "small amount" from one  $z$  level to the next. By this we mean that the function  $f$  in (16) should undergo a phase change less than one radian over a distance  $2\delta z$ :

$$|2p_z \delta z| \leq 1 , \quad (31)$$

where the limiting form (15) is used for  $p_z$ .

Thus we have

$$\text{RESOLUTION REQUIREMENT: } \delta z \leq k_o^{-1} \left( |x_1| + \frac{1}{k_o^2 L^2} \right)^{-1} \quad (32)$$

We have made changes in going to (15) to (33) to account for the fact that  $x_1$  may be positive or negative. The ratio of the largest  $\delta z$  permitted by the resolution condition to the largest value allowed by the stability condition is

$$\frac{\delta z_R}{\delta z_S} = \frac{8/\delta x^2 + k_o^2 |x_1|}{2(1/L^2 + k_o^2 |x_1|)} , \quad (33)$$

where  $\delta z_R$  and  $\delta z_S$  are taken from (32) and (31) respectively. For small

$x_1$ , this ratio tends to  $4L^2/\delta x^2$ . This value is by assumption greater than one for all cases that can be considered within the framework of a discrete point representation. When the  $x_1$  term dominates, (33) tends toward the value  $1/2$ . To insure stability and adequate resolution, we take the lesser of (30) and (32) for  $\delta z$ . This can be summarized as follows:

When  $k_o^2 |x_1| \leq 8/\delta x^2 - 2/L^2$  use (30)  
 "      >      "      use (32).

We have treated  $|x_1|$  as a constant in writing (30) - (33). In practice, one would use the maximum value at a given  $z$  level to determine the stepsize  $\delta z$ .

### C. BOUNDARY CONDITIONS

In the examples to be presented in the next section we have used a very simple (although arbitrary) algorithm for defining the Laplacian operator  $\nabla_{\perp}^2$  at the edges of the mesh. Namely, we have set the normal second derivative equal to zero at all locations one cell from the boundary. We confine the calculation to the interior mesh. Suppose that the  $(x,y)$  mesh consists of  $NX$  by  $NY$  points. Then for all  $J$  and  $K$  we impose the condition

$$f(1,J,K) = 2f(2,J,K) - f(3,J,K) \quad (34)$$

$$f(NX,J,K) = 2f(NX-1,J,K) - f(NX-2,J,K) .$$

A straightforward extension of (34) defines  $f$  for  $J = 1$  and  $NY$ . In practice, we use (18) and (19) to update  $f$  on the interior mesh  $I = 2$  to  $NX-1$ ,  $J = 2$  to  $NY-1$ , and define  $f$  on the boundaries with (34). We have so far not noticed any stability or accuracy problems resulting

from (34).

#### D. RESULTS FROM THE PEP CODE

We have two comparisons to present between numerical solutions to (18) and published results obtained by other means. We have carried out the numerical procedure defined in (18) and (19) and included certain diagnostic features in a "Parabolic Equation Propagation" code, whose acronym is conveniently PEP. Values for the real and imaginary parts of  $f$  are assigned at some initial  $z$  level. The PEP code steps (18) forward, and at specified intervals computes "scintillation indices," phase variances in radians, and power variances in decibels.

The scintillation index of greatest interest is

$$s_4(z) = \sqrt{\frac{\langle |f|^4 \rangle - \langle |f|^2 \rangle^2}{\langle |f|^2 \rangle}} , \quad (35)$$

where the bracket  $\langle \rangle$  refers to an average over  $x$  and  $y$ , with  $z$  fixed.

The phase and power variances are respectively

$$\sigma_{\phi}^2(z) = \langle \phi^2 \rangle - \langle \phi \rangle^2 \quad (36)$$

where

$$\phi = \tan^{-1} f_i/f_r ; \text{ and}$$

$$\sigma_x^2(z) = 100 \langle (\log_{10} |f|^2)^2 \rangle - 100 \langle \log_{10} |f|^2 \rangle^2 . \quad (37)$$

The notation conflict between the power variance  $\sigma_x^2$  and the susceptibility  $\chi$  is a result of established conventions in ionospheric and plasma physics literature.

## 1. Focusing by a Gaussian Lens

First we consider a wave incident on a two dimensional lens  $(x, z)$  whose thickness in terms of phase delay is

$$\Phi(x, 0) = 10 \exp(-x/\ell)^2 \quad (38)$$

radians. This problem has been examined numerically by Buckley<sup>5</sup> using a small angle diffraction approach. Our approach is to solve the initial value problem (16) with  $x_1 = 0$  everywhere below the lens ( $z \leq 0$ ), and with initial conditions

$$f(x, 0) = e^{i\Phi(x, 0)}. \quad (39)$$

The two dimensional problem was integrated according to the prescription (18) - (19) with the J index suppressed. Numerical values used for the integration were:  $\delta x = .05$ ,  $\delta z = 0.314159$ ,  $\lambda = .01$ ,  $\ell = 1$ ,  $NZ = 402$ , and  $NX = 82$ . Results for the "power"  $|E(x, z)|^2 = |f(x, z)|^2$  are in Figure 3. The qualitative agreement with Buckley's result<sup>5</sup> is quite satisfactory. Z in Figure 3 is a dimensionless coordinate which can be used to scale equation (16):

$$Z = z/k\ell^2 \quad (40)$$

## 2. Diffraction from a Random Phase Screen

Let us consider a three dimensional problem in which the initial phase  $\Phi(x, y, 0)$  is a random function of x and y with Gaussian autocorrelation:

$$\langle \Phi(x, y, 0) \Phi(x + \xi, y + \eta, 0) \rangle = \Phi_0^2 e^{-\xi^2 + \eta^2 / r_0^2}. \quad (41)$$

Such a function can be generated numerically by Fourier transforming the desired spatial autocorrelation function, multiplying each Fourier

component by a random phase factor  $e^{i\omega}$ , and then transforming back into xy space. In this prescription,  $\omega$  is an arbitrarily generated number ranging from 0 to  $2\pi$ . To insure that  $\Phi$  is real, one can assign  $\omega$  arbitrarily in one half of the transform space ( $k_x, k_y$ ) and then set  $\omega(-k_x, -k_y) = -\omega(k_x, k_y)$ .

We have generated a function satisfying (41) to use as an initial condition for (16). We initialize the calculation with

$$f(x, y, \omega) = e^{i\Phi(x, y, \omega)} \quad (42)$$

and integrate forward into free space ( $x = 0$ ). Four curves showing computed values of  $S_4$  versus propagation distance for different values of  $\Phi_0$  appear in Figure 4. The dots are from the calculation, and the solid curves are the results of Mercier<sup>6</sup> plotted in the format of Briggs and Parkin<sup>7</sup>. The results are in good agreement with the solid curves. The data used to generate these results were  $\delta x = .002$ ,  $\delta z = .015$ ,  $\lambda = .0001$ ,  $r_0 = .01$ ,  $NX = 27$ ,  $NY = 27$ , and  $NZ = 102$ .

#### SUMMARY

We have described a set of coupled linear equations (18) which result from the wave equation (1) in the parabolic approximation. Equations (18) differ from the usual "parabolic equation" only in that the index of refraction is allowed to vary slightly along an assumed propagation direction as part of the background or unscattered state. A rough estimate of the error introduced by the parabolic approximation is given after (16). We have constructed the PEP code for finite difference solution of (18) using the centered leapfrog scheme (19). The stability criterion for the scheme is (30).

Results from the PEP code are in good agreement with those obtained by different means for refraction due to a Gaussian lens and for refraction due to a random phase screen. These two examples involve propagation into a vacuum of an initially specified wave. Results for propagation within a scattering medium will be given elsewhere.

#### REFERENCES

1. K. C. Yeh and C. H. Liu, Theory of Ionospheric Waves (Academic Press, New York, 1972), Chap. 6
2. P. M. Morse, Theoretical Acoustics (McGraw Hill, New York, 1968), Equation 8.1.12.
3. Y. N. Barabanenkov, Y. A. Kravtsov, S. M. Rytov and V. I. Tatarskii, Soviet Phys. Uspekhi (English translation) 13, 551, 1971.
4. R. H. Hardin and F. D. Tappert, "Analysis, Simulation, and Models of Ionospheric Scintillation," Bell Laboratories Report, March 1, 1974.
5. R. Buckley, J. Atmos. Terr. Phys. 37, 1431, 1975.
6. R. P. Mercier, Proc. Camb. Phil. Soc. 58, 382, 1962.
7. B. H. Briggs and I. A. Parkin, J. Atmos. Terr. Phys. 25, 339, 1963.

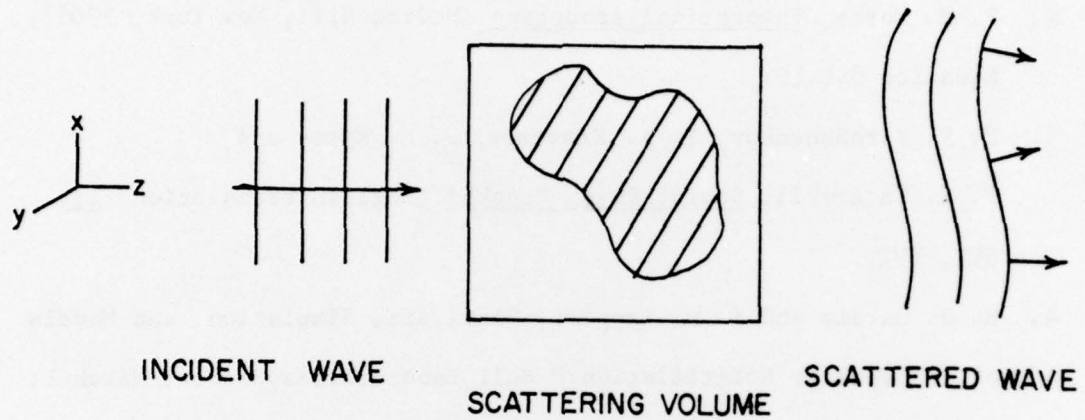


Fig. 1 — A wave incident along the z direction is scattered by inhomogeneities in the scattering volume

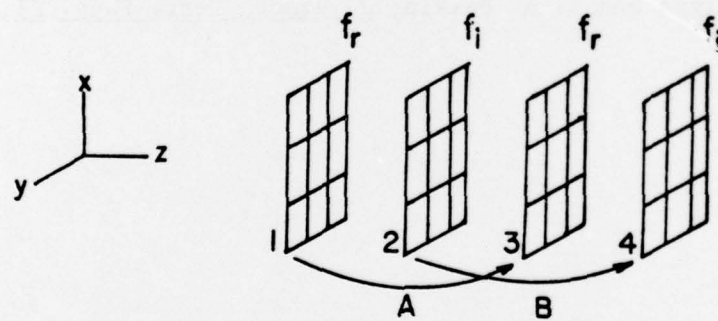


Fig. 2 — Leapfrog difference scheme. Step A updates the real part of  $f$  from plane 1 to plane 3 according to (18) and (19). Then Step B updates the imaginary part of  $f$  from plane 2 to plane 4.

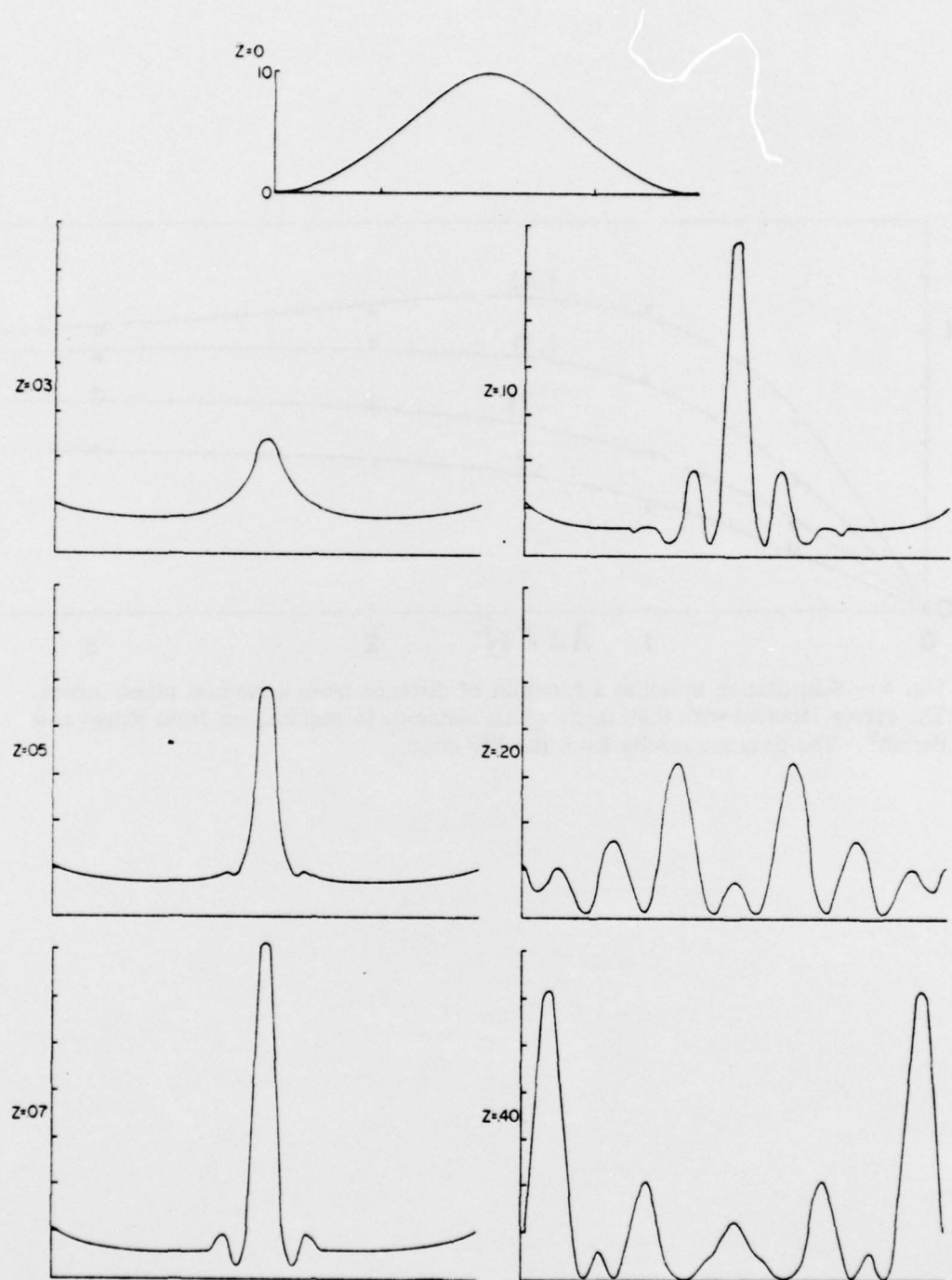


Fig. 3 — Diffraction due to a Gaussian lens. At the top is phase delay in radians for  $Z = 0$ . The other curves are the power,  $|f|^2$ , at distances  $Z$  (see (40)) from the lens.

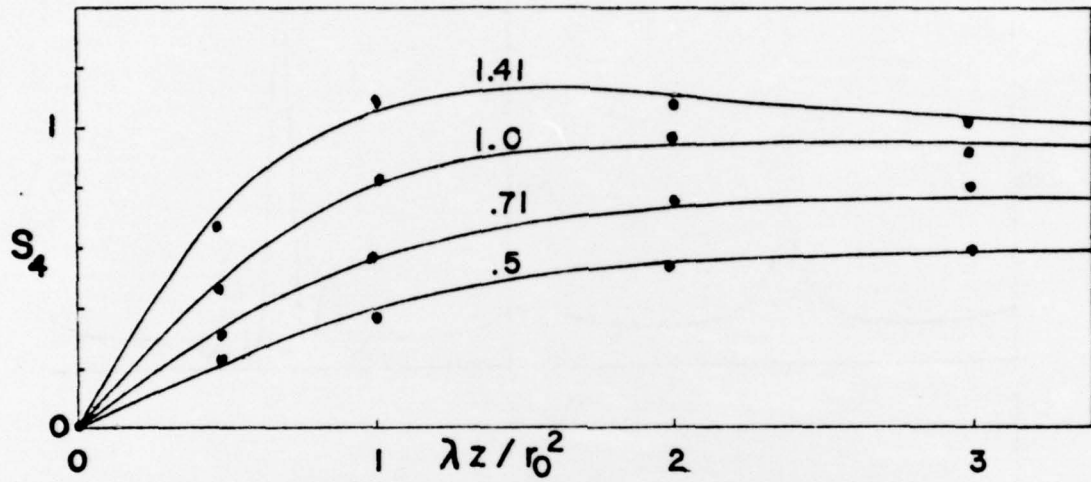


Fig. 4 — Scintillation index as a function of distance from a random phase screen. The curves, labelled with their initial phase variances in radians, are from Briggs and Parkin<sup>7</sup>. The dots are results from the PIP code.

DISTRIBUTION LIST

Advanced Research Projects Agency (ARPA)  
Strategic Technology Office  
Arlington, Virginia

Capt. Donald M. LeVine

Naval Research Laboratory  
Washington, D. C. 20375

Dr. P. Mange  
Dr. E. Peterkin  
Dr. R. Meier  
Dr. E. Szuszczewicz -- Code 7127  
Dr. Timothy Coffey -- Code 7700 (20 copies)  
Dr. J. Goodman -- Code 7950

Science Applications, Inc.  
1250 Prospect Plaza  
La Jolla, California 92037

Dr. D. A. Hamlin  
Dr. L. Linson  
Dr. D. Sachs

Director of Space and Environmental Laboratory  
NOAA  
Boulder, Colorado 80302

Dr. A. Glenn Jean  
Dr. G. W. Adams  
Dr. D. N. Anderson  
Dr. K. Davies  
Dr. R. F. Donnelly

A. F. Cambridge Research Laboratories  
L. G. Hanscom Field  
Bedford, Mass. 01730

Dr. T. Elkins  
Dr. W. Swider  
Mrs. R. Sagalyn  
Dr. J. M. Forbes  
Dr. T. J. Keneshea  
Dr. J. Aarons

Office of Naval Research  
800 North Quincy Street  
Arlington, Virginia 22217

Dr. J. G. Dardis  
Dr. H. Mullaney

Commander  
Naval Electronics Laboratory Center  
San Diego, California 92152

Dr. M. Bleiweiss  
Dr. I. Rothmuller  
Dr. V. Hildebrand  
Mr. R. Rose

U. S. Army Aberdeen Research and Development Center  
Ballistic Research Laboratory  
Aberdeen, Maryland

Dr. F. Niles  
Dr. J. Heimerl

Commander  
Naval Air Systems Command  
Department of the Navy  
Washington, D. C. 20360

Dr. T. Czuba

Harvard University  
Harvard Square  
Cambridge, Mass.

Dr. M. B. McElroy  
Dr. R. Lindzen

Pennsylvania State University  
University Park, Pennsylvania 16802

Dr. J. S. Nisbet  
Dr. P. R. Rohrbaugh  
Dr. D. E. Baran  
Dr. L. A. Carpenter  
Dr. M. Lee  
Dr. R. Divany  
Dr. P. Bennett  
Dr. E. Klevans

University of California, Los Angeles  
405 Hillgard Avenue  
La Jolla, California 90024

Dr. F. V. Coroniti  
Dr. C. Kennel

University of California, San Diego  
P. O. Box 109  
La Jolla, California 92037

Dr. P. M. Banks

Utah State University  
4th N. and 8th E. Streets  
Logan, Utah 84322

Dr. R. Harris  
Dr. V. Peterson  
Dr. R. Megill

Cornell University  
Ithaca, New York 14850

Dr. W. E. Swartz  
Dr. R. Sudan  
Dr. D. Farley  
Dr. M. Kelley

NASA  
Goddard Space Flight Center  
Greenbelt, Maryland 20771

Dr. S. Chandra  
Dr. K. Maedo

Princeton University  
Plasma Physics Laboratory  
Princeton, New Jersey 08540

Dr. F. Perkins

Institute for Defense Analysis  
400 Army/Navy Drive  
Arlington, Virginia 22202

Dr. E. Bauer